Weierstraß-Institut

für Angewandte Analysis und Stochastik

im Forschungsverbund Berlin e. V.

Preprint ISSN 2198 – 5855

A phase-field model for solid-state dewetting and its sharp-interface limit

Marion Dziwnik[1], Andreas Münch[2], Barbara Wagner[1,3]

submitted: December 12, 2014

[1] Institute of Mathematics
Technische Universität Berlin
Str. des 17. Juni 136
10623 Berlin
Germany
E-Mail: dziwnik@math.tu-berlin.de

[2] Mathematical Institute
24-29 St Giles'
University of Oxford
Oxford, OX1 3LB
UK
E-Mail: muench@maths.ox.ac.uk

[3] Weierstrass Institute
Mohrenstr. 39
10117 Berlin
Germany
E-Mail: barbara.wagner@wias-berlin.de

No. 2048
Berlin 2014

2010 *Mathematics Subject Classification.* 34E13, 74N20, 74E10.

Key words and phrases. Phase-field model, matched asymptotic expansions, sharp interface model, free boundaries, dewetting solid films.

The authors are very grateful to Dirk Peschka for fruitful discussions on the numerical part of our study. MD and BW gratefully acknowledges the support by the Federal Ministry of Education (BMBF) and the state government of Berlin (SENBWF) in the framework of the program *Spitzenforschung und Innovation in den Neuen Ländern* (Grant Number 03IS2151).

Edited by
Weierstraß-Institut für Angewandte Analysis und Stochastik (WIAS)
Mohrenstraße 39
10117 Berlin
Germany

Fax: +49 30 2044975
E-Mail: preprint@wias-berlin.de
World Wide Web: http://www.wias-berlin.de/

Abstract

We propose a phase field model for solid state dewetting in form of a Cahn-Hilliard equation with weakly anisotropic surface energy and a degenerate mobility together with a free boundary condition at the film-substrate contact line. We derive the corresponding sharp interface limit via matched asymptotic analysis involving multiple inner layers. The resulting sharp interface model is consistent with the pure surface diffusion model. In addition, we show that the natural boundary conditions, as indicated from the first variation of the total free energy, imply a contact angle condition for the dewetting front, which, in the isotropic case, is consistent with the well-known Young's equation.

1 Introduction

Dewetting of solid films is one of the important processes used for nanostructuring and functionalizing surfaces for a variety of technological applications, such as for example in thin-film solar cells and other optoelectronic devices. Examples can be found in [8, 10, 30] and for a recent review we refer to Thompson [34]. Typically, the dewetting scenario begins with the formation of a three-phase contact line between the thin solid film, the solid substrate and the surrounding vapor phase. The subsequent retraction of the film leads to the formation of a rim that eventually destabilizes into nano- or micro- islands [35].

While this process is very similar to the dewetting of liquid thin films and investigated in detail in [1, 9, 18] and recently reviewed in [7], the physical mechanisms for the mass transport underlying solid film dewetting is quite different and is based on capillarity driven surface diffusion [17, 35, 39]. In addition, for solid films further properties such as anisotropy of its surface energy can dominate the dynamics [11, 36, 42]. This can have important implication on the stability of the moving three-phase contact-line, where vapor, solid film and substrate meet. For the equilibrium state the shape of a nano- or micro crystal in contact with a substrate has been systematically derived as well as experimentally validated in [20, 37].

Since the dynamical dewetting process usually involves a succession of topological transitions of the thin dewetting film the phase field framework provides an adequate modeling approach for a continuum description. In particular, for large-scale numerical simulations the evolving complex geometries such as the creation and vanishing of interfaces, occur naturally as part of the solution. This is in contrast to interface tracking methods used for the corresponding sharp-interface models. However, establishing the correct correspondence between the phase-field and sharp-interface models can emerge as a non-trivial and subtel asymptotic problem and this is the main focus of our present study.

For the isotropic case a phase-field model for solid phase dewetting has been proposed by Jiang et al. [16], where a phase-field function $u = u(\mathbf{x})$ that lives on the domain Ω which includes film-vapor interfaces, where $u(\mathbf{x}) = 0$, has been defined such that $u(\mathbf{x}) > 0$ inside the film and $u(\mathbf{x}) < 0$ inside the vapor phase. For this phase-field variable the total free energy W combines the Ginzburg-Landau free energy density for the film-vapor system and the energy density of the wall

$$W = \int_{\Omega} f_{FV}\, d\Omega \, + \, \int_{\gamma_w} f_w \, d\Gamma_w, \tag{1}$$

where

$$f_{FV} \equiv \lambda \left(F(u) + \frac{\varepsilon^2}{2} |\nabla u| \right) \quad \text{and} \quad f_w \equiv \frac{\gamma_{VS} + \gamma_{FS}}{2} - \frac{u(3-u^2)}{4}(\gamma_{VS} - \gamma_{FS}) \tag{2}$$

with the constants ϵ denoting the interface width and λ the mixing energy density. While the expression for f_{FV} is well-known, the less familar expression for the wall-energy is found from the conditions that $f_w = \gamma_{VS}$, $f_w' = 0$ for $u = -1$ and $f_w = \gamma_{FS}$, $f_w' = 0$ for $u = 1$ as has been first constructed in [15, 41] and discussed further in [14] for a problem of two-phase dewetting. Physically more meaningful but more involved expressions for the wall energy can be found in [29].

A derivation via the first variational derivative of the total free energy functional with respect to u then yields the correcponding chemical potential $\mu = 1/\lambda \; \delta W/\delta u$ so that by making use of the fact that u is a conserved order parameter, the Cahn-Hilliard equation [26]

$$\partial_t u = \nabla \cdot \mathbf{j}, \qquad \mathbf{j} = M(u) \nabla \mu, \qquad \mu = F'(u) - \epsilon^2 \Delta u, \tag{3}$$

is obtained, together with the natural (no-material flux) boundary condition $\partial \mu / \partial \mathbf{n} = 0$ on $\partial \Omega$. Here, $M(u)$ denotes the mobility, $\mathbf{j}$ the flux and F the homogeneous free energy. In Jiang et al. [16] the choice was $M(u) = 1 - u^2$ and $F(u) = 1/2(1-u^2)^2$.

The sharp-interface limits of these phase-field models require careful consideration in order to predict the correct physical properties. In particular, in view of mobility M and homogeneous free energy F different combinations have been investigated in the literature and the results show that appropriate choices do significantly affect the corresponding sharp-interface limit, see [26]. In [32] Taylor & Cahn show in general how sharp-interface and diffuse-interface motion laws can be linked by being gradient flows for analogous inner products. One of the first systematic asymptotic studies was done by Pego [28], where he showed that for the combination

$$M(u) = M_0(u) \; \equiv 1, \tag{4a}$$

$$F(u) = F_0(u) \; \equiv \frac{1}{2}(1-u^2)^2 \tag{4b}$$

the sharp interface limit $\epsilon \to 0$ leads to the well known Mullins-Sekerka problem [24]. His asymptotic technique has been frequently adapted by other authors in order to show that pure surface diffusion flux is recovered for corresponding choices of free energy F and mobility M as intended.
The choice considered by Pego (4) can be considered as an approximation of the

Cahn-Hilliard equation (3) with a concentration dependent mobility and a logarithmic free energy [26]

$$M(u) = M_1(u) \equiv 1 - u^2, \tag{5a}$$

$$F(u) = F_l(u) \equiv \frac{T}{2}((1+u)\ln(1+u) + (1-u)\ln(1-u)) + F_0(u), \tag{5b}$$

in the shallow quench limit, $T \to 1$, where T is the temperature. Cahn et al. [6] studied combination (5) in the deep quench limit, $T = 0$, and their analysis yields that (3) together with (5) reduces to a model for surface diffusion in the limit $\epsilon \to 0$.
Other combinations of free energy and mobility have frequently been applied in the literature in order to approach surface diffusion, often simply to circumvent the numerical difficulties of the logarithmic potential. Typical approximations are for example the biquadratic free energy such as F_0 in combination with a degenerate mobility such as M_1 or doubly degenerate mobility as $M_2(u) = (1-u^2)^2$, see for example [16, 31]. However, some of these models do not reliably approach surface diffusion as intended and has been criticized in the literature in particular in Guggenberger et al. [13]. Only recently this was shown in [22], where via a systematic asymptotic analysis that in addition takes account of contributions from exponential asymptotics, showed that for M_1 combined with the double-well potential F_0 bulk diffusion will in fact enter into the interfacial mass flux at the same order as surface diffusion and thereby would predict different physical processes. As a consequence of this, we show in our analysis here that the doubly degenerate mobility will yield the correct limiting sharp-interface model.

In addition we include in our Phase-field model also anisotropic surface energy $\gamma(\theta)$, where θ is the interface orientation angle. We note that anisotropic surface energy may lead to an ill-posed problem when there are missing orientations in the corresponding Wulff shape, because then the surface energy is non-convex [12, 38]. In the two-dimensional case this is equivalent to the surface tension $\gamma(\theta) + \gamma''(\theta)$ having a sign change and this case is referred to as strongly anisotropic. The topic of strong anisotropy in the Cahn-Hilliard equation was considered by Cahn and Taylor [5] where they suggested to convexify the gradient energy to keep the equations well-posed. Another convexication scheme was proposed by Eggleston et al. [12], where corresponding equilibrium solutions were remarkably close to the sharp-interface Wulff shapes, but did not conserve mass. Moreover, in a work by Lowengrub et al. [38], an efficient, second-order accurate and adaptive finite-difference methods is presented to solve the regularized, anisotropic Cahn -Hilliard equation in two and three dimensions.

When investigating the sharp-interface limit for dewetting film we also have to take into account the limit towards adequate boundary conditions at triple junctions for the anisotropic Cahn-Hilliard equation. Other studies that deal with the boundary conditions at triple junctions have considered the isotropic Cahn-Hilliard equation [25], where the ideas of [3] are adapted in order to show that in the asymptotic limit the boundary condition leads to Youngs law at triple junctions [40], i.e.

$$\gamma_{VS} - \gamma_{FS} = \gamma_{FV} \cos\theta_C, \tag{6}$$

where γ_{VS}, γ_{FS} and γ_{FV} are the interface energy densities describing the interfaces between vapor and substrate, film and substrate, and film and vapor, respectively, θ_C

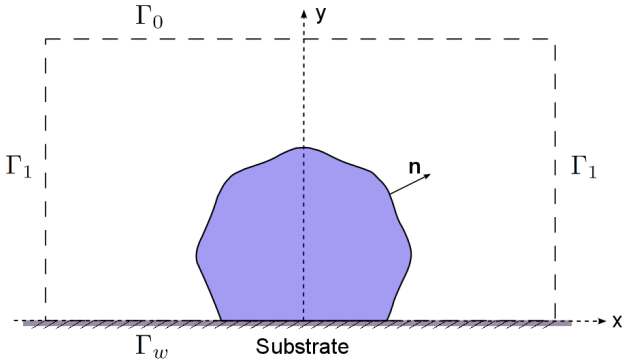

Figure 1: A sketch of the model domain.

and the equilibrium contact angle. Of particular interest in our study is the technique as well as the geometry presented in [27], in order to study the asymptotic behavior at the contact line for our problem.

The paper is organized as follows. First we propose a phase field model for solving the anisotropic surface-diffusion dewetting problem. In section 3 we derive the corresponding sharp-interface limit in the weakly anisotropic case and inside the model domain which confirms the approach of surface diffusion for the present choice of mobility M and free energy F. In section 4 we deal with the corresponding boundary condition at the triple junction and apply an appropriate asymptotic method in order to derive the anisotropic contact angle boundary condition.

2 Problem formulation

Considering a one-dimensional film/vapor interface, we define the domain Ω to be a two-dimensional rectangular box around this interface with boundary $\partial\Omega = \Gamma_0 \cup \Gamma_1 \cup \Gamma_w$ (see Fig. 1). Then for the phase-field function u as defined in the introduction the energy functional W may be extended following the approach by Kobayashi [19] and similarly [33, 38], and we consider an anisotropic free energy functional of the form

$$f_{FV}(u, \nabla u) = \lambda\left(F(u) + \frac{\epsilon^2}{2}\gamma(-\nabla u)^2|\nabla u|^2\right), \tag{7}$$

where $F(u)$ is the homogeneous free energy, $\gamma : \mathbb{R}^2 \to \mathbb{R}^+$ is the anisotropic interface energy between film and vapor and λ represents the mixing energy density. Note that γ depends on the direction of the outer normal vector at the interface and this direction is represented by $-\nabla u$.
In this paper, we will consider the sharp interface limit for the case where the homogeneous free energy is the double well potential (4b). Moreover, following [19] we assume that the anisotropy function satisfies $\gamma(\lambda\mathbf{v}) = \gamma(\mathbf{v})$, for $\lambda > 0$ and $\mathbf{v} \in \mathbf{R}^2$, and exploit that in a two dimensional space, the direction $-\nabla u$ in $\gamma(-\nabla u)$ may be written in polar coordinates. Thus there is an equivalent representation of γ which only depends on θ, the angle of orientation of the interface relative to the positive x-axis [19]. In order to determine θ in $[-\pi, \pi]$ we chose the following common variation

of the arctangent function

$$\theta := \arctan 2(u_y, u_x) = \begin{cases} \arctan \frac{u_y}{u_x} & , \text{ for } u_x > 0 \\ \arctan \frac{u_y}{u_x} + \pi & , \text{ for } u_x < 0, u_y \geq 0 \\ \arctan \frac{u_y}{u_x} - \pi & , \text{ for } u_x < 0, u_y < 0 \\ + \frac{\pi}{2} & , \text{ for } u_x = 0, u_y > 0 \\ - \frac{\pi}{2} & , \text{ for } u_x = 0, u_y < 0 \\ 0 & , \text{ for } u_x = 0, u_y = 0 \end{cases} \tag{8}$$

and consider the following form of γ

$$\gamma = \gamma(\theta) = \gamma\left(\arctan 2(u_y, u_x)\right).$$

Note that, since π and $-\pi$ correspond to the same direction, we have to postulate that $\gamma(\pi) = \gamma(-\pi)$. Moreover we suppose that the system is weakly anisotropic, i.e.

$$\gamma(\theta) + \gamma''(\theta) > 0, \tag{9}$$

for all $\theta \in [-\pi, \pi]$, which ensures that the film-vapor interface is always smooth during the evolution and the anisotropic model is mathematically well-posed [12].
As before we assume for the wall energy density [15]

$$f_w(u) \ = \ \frac{\gamma_{VS} \ + \ \gamma_{FS}}{2} \ - \ \frac{u(3-u^2)}{4}(\gamma_{VS} - \gamma_{FS}), \tag{10}$$

which satisfies $f_w = \gamma_{VS}$ and $f_w' = 0$ when $u = -1$ and $f_w = \gamma_{FS}$ and $f_w' = 0$ when $u = 1$. It follows that the variational derivative of the energy functional W^ϵ with respect to u is

$$\frac{1}{\lambda}\frac{\delta W^\epsilon}{\delta u} = F'(u) - \epsilon^2 \nabla \left(\gamma\gamma' \begin{pmatrix} -u_y \\ u_x \end{pmatrix} + \gamma^2 \nabla u \right) \tag{11}$$

which suggests the following natural boundary conditions

$$\epsilon \, \mathbf{m} \cdot \left[\gamma(\theta)\gamma'(\theta) \begin{pmatrix} -u_y \\ u_x \end{pmatrix} + \gamma(\theta)^2 \nabla u \right] + \frac{f_w'}{\lambda} = 0 \tag{12}$$

on Γ_w, and

$$\mathbf{m} \cdot \left[\gamma(\theta)\gamma'(\theta) \begin{pmatrix} -u_y \\ u_x \end{pmatrix} + \gamma(\theta)^2 \nabla u \right] = 0 \tag{13}$$

on $\partial\Omega \setminus \Gamma_w$, where $\mathbf{m}$ is the unit outward pointing normal vector onto Ω.
We assume that the order parameter u is conserved and define the mass flux of u to be

$$\mathbf{j} = M(u)\nabla\mu, \tag{14}$$

where the chemical potential μ is the first variational derivative of W^ϵ with respect to u

$$\mu(u) := F'(u) - \epsilon^2 \nabla \left(\gamma\gamma' \begin{pmatrix} -u_y \\ u_x \end{pmatrix} + \gamma^2 \nabla u \right) \tag{15}$$

and we chose the biquadratic diffusional mobility $M(u)$ to be

$$M(u) = \left(1 - u^2\right)^2. \tag{16}$$

Fick's second law then yields the anisotropic Cahn-Hilliard equation

$$\partial_t u = \nabla \cdot \mathbf{j}, \qquad \mathbf{j} = M(u)\nabla\mu, \qquad \mu = F'(u) - \epsilon^2 \nabla \left(\gamma\gamma' \begin{pmatrix} -u_y \\ u_x \end{pmatrix} + \gamma^2 \nabla u \right), \quad (17a)$$

subject to the following boundary conditions

$$\epsilon\, \mathbf{m} \cdot \left[\gamma(\theta)\gamma'(\theta) \begin{pmatrix} -u_y \\ u_x \end{pmatrix} + \gamma(\theta)^2 \nabla u \right] + \frac{f_w'}{\lambda} = 0, \qquad \mathbf{m} \cdot (M(u)\nabla\mu) = 0, \quad (17b)$$

on Γ_w and

$$\mathbf{m} \cdot \nabla u = 0, \qquad \mathbf{m} \cdot (M(u)\nabla\mu) = 0, \quad (17c)$$

on $\partial\Omega \backslash \Gamma_w$. The aim of this paper is to study the sharp interface limit for the anisotropic phase field model (17) with mobility M defined by (16) and free energy F defined by (4b) on a long time scale, when the solution only changes slowly in time.

3 Dynamics away from the solid boundary

We now apply the method of matched asymptotic expansions in order to study the long time behaviour of (17) in the limit $\epsilon \to 0$ and capture the contribution from surface diffusion. Observing that the evolution of the order parameter occurs at an $O(1/\epsilon^2)$ time scale (see [22]), we suggest to rescale time via $\tau = \epsilon^2 t$, so that the Cahn-Hilliard equation reads

$$\epsilon^2 \partial_\tau u = \nabla \cdot \mathbf{j}, \qquad \mathbf{j} = M(u)\nabla\mu, \qquad \mu = F'(u) - \epsilon^2 \nabla \left(\gamma\gamma' \begin{pmatrix} -u_y \\ u_x \end{pmatrix} + \gamma^2 \nabla u \right), \quad (18)$$

with mobility M defined by (16) and free energy F defined by (4b) and boundary conditions (17b) and (17c).

We first study the asymptotic behaviour of the solution away from the solid boundary at $y = 0$, where the boundary condition (17c) is not present and we only have the condition

$$\mathbf{m} \cdot \nabla u = 0, \qquad \mathbf{m} \cdot (M(u)\nabla\mu) = 0, \quad (19)$$

on $\partial\Omega$.

Motivated by [22], we consider three layers, an outer layer away from the contact line, an interior layer about the interface, and further, a second interior layer where u is below and arbitrarily close to 1. The reason for considering this second interior layer is, that in inner coordinates about the interface, the solution is similar to a $\tanh$ function, which differs from its asymptotic value -1 as the inner coordinate tends to $-\infty$ by a small amount ϵ. Taking the exponential representation of $\tanh$ this distance can be measured to be of $O(\ln(1/\epsilon))$, which means that the free boundary, where $u = 1$, is asymptotically far away from the interface. Consequently a second interior layer must match between the classic outer and inner solution.

3.1 Outer problem

For the outer expansions, we will use

$$\begin{aligned} u &= u_0 + \epsilon u_1 + \epsilon^2 u_2 ..., \\ \mu &= \mu_0 + \epsilon \mu_1 + \epsilon^2 \mu_2 ..., \\ \mathbf{j} &= \mathbf{j}_0 + \epsilon \mathbf{j}_1 + \epsilon^2 \mathbf{j}_2 .... \end{aligned} \tag{20}$$

which suggests the following expansions for $M(u)$ and $F(u)$

$$M(u) = M(u_0) + \epsilon M'(u_0) u_1 + \epsilon^2 \left(\frac{1}{2} M''(u_0) u_1^2 + M'(u_0) u_2 \right) + O(\epsilon^3)$$
$$F'(u) = F'(u_0) + \epsilon F''(u_0) u_1 + \epsilon^2 \left(\frac{1}{2} F'''(u_0) u_1^2 + F''(u_0) u_2 \right) + O(\epsilon^3).$$

Moreover we have

$$u_0 = -1, \qquad \mu_0 = 0 \tag{21}$$

as we suppose that the "phase is outside the solid film.

3.2 Inner problem

Similar as in [22, 28], we define the inner layer in a coordinate system relative to the interface

$$\mathbf{x} = \mathbf{R}(s, \tau) + \epsilon \rho \, \mathbf{n}(s, \tau) \tag{22}$$

where $\mathbf{R}$ is the position of the interface and $\mathbf{n} = (n_1, n_2)^T$ is the unit outward normal onto the film/vapor interface. The position of the interface is defined by

$$u(\mathbf{R}, t) = 0, \tag{23}$$

and the gradient operator in these curvilinear coordinates reads

$$\nabla = \mathbf{n} \epsilon^{-1} \partial_\rho + \frac{1}{1 + \epsilon \rho \kappa} \mathbf{t} \partial_s, \tag{24}$$

where $\mathbf{t} = (t_1, t_2)^T$ is the unit tangent, and according to the orientation of $\mathbf{n}$ we have $\mathbf{t} = (n_2, -n_1)^T$.
For the inner expansions, we will use

$$\begin{aligned} U &= U_0 + \epsilon U_1 + \epsilon^2 U_2 ..., \\ \eta &= \eta_0 + \epsilon \eta_1 + \epsilon^2 \eta_2 ..., \\ \mathbf{J} &= \epsilon^{-1} \mathbf{J}_{-1} + \mathbf{J}_0 + \epsilon \mathbf{J}_1 + \epsilon^2 \mathbf{J}_2 .... \end{aligned} \tag{25}$$

and moreover introduce expansions for θ and γ respectively, as these are relevant for the first three orders of the inner problem

$$\begin{aligned} \theta &= \theta_0 + \epsilon \theta_1 + \epsilon^2 \theta_2 ..., \\ \gamma &= \gamma(\theta_0) + \epsilon \gamma'(\theta_0) \theta_1 + \epsilon^2 \left(\frac{1}{2} \gamma''(\theta_0) \theta_1^2 + \gamma'(\theta_0) \theta_2 \right) .... \end{aligned} \tag{26}$$

Notice that in inner coordinates and exploiting $(t_1, t_2) = (n_2, -n_1)$ we have

$$\frac{u_y}{u_x} \sim \frac{n_2}{n_1} - \epsilon \frac{U_s}{n_1^2 U_\rho} + O(\epsilon^2)$$

for $n_1 \neq 0$, such that a Taylor-expansion of θ at $\epsilon = 0$ leads to

$$\theta = \arctan 2\,(n_2, n_1) + O(\epsilon). \tag{27a}$$

On the other hand, for $n_1 = 0$, we have

$$\frac{u_y}{u_x} \sim \epsilon^{-1} \frac{U_\rho}{U_s} + O(1)$$

such that in the limit $\epsilon \to 0$ the Taylor-expansion leads to

$$\theta = \operatorname{sign}\left(\frac{U_\rho}{U_s}\right) \frac{\pi}{2} + O(\epsilon). \tag{27b}$$

which all together reveals that the leading order $\theta_0 := \arctan 2(n_2/n_1)$ is independent of ρ and denoting $\gamma_0 := \gamma(\theta_0)$ the same holds true for the leading order γ_0.
Applying these inner expansions in (18) we find that, the first two equations combined become

$$\epsilon^2 \partial_\tau U - \epsilon v_n \partial_\rho U = \nabla(M(U)\nabla\eta) \tag{28}$$

with $v_n = \mathbf{R}_\tau \cdot \mathbf{n}$ and where

$$\begin{aligned}\nabla \cdot (M(U)\nabla) =& \epsilon^{-2} \partial_\rho M(U_0) \partial_\rho + \epsilon^{-1} \Big[\partial_\rho \Big(\kappa\rho M(U_0) + M'(U_0) U_1 \Big) \partial_\rho - \kappa\rho \partial_\rho M(U_0) \partial_\rho \Big] \\ &+ \Big[\kappa^2 \rho^2 \partial_\rho M(U_0) \partial_r ho - \kappa\rho \partial_\rho \Big(\kappa\rho M(U_0) + M'(U_0) U_1 \Big) \partial_\rho \\ &+ \Big(\kappa\rho M'(U_0) U_1 + \frac{1}{2} M''(U_0) U_1^2 + M'(U_0) U_2 \Big) \partial_\rho + \partial_s M(U_0) \partial_s \Big] + O(\epsilon).\end{aligned} \tag{29}$$

Taking only the first equation in (18) we have

$$\epsilon^2 \partial_\tau U - \epsilon v_n \partial_\rho U = \frac{1}{1 + \epsilon\rho\kappa} \left[\epsilon^{-1} \partial_\rho \Big((1 + \epsilon\rho\kappa) J_n \Big) + \partial_s \left(\frac{1}{1 - \epsilon\rho\kappa} J_s \right) \right]$$

so that in inner coordinates we will only need to know the normal component $J_n = \mathbf{n} \cdot \mathbf{J}$ which can be expanded as

$$\begin{aligned} J_n &= \frac{M(U)}{\epsilon} \partial_\rho \eta \\ &= \epsilon^{-1} M(U_0) \partial_\rho \eta_0 + M'(U_0) U_1 \partial_\rho \eta_0 + M(U_0) \partial_\rho \eta_1 \\ &\quad + \epsilon \Big[M(U_0) \partial_\rho \eta_2 + M'(U_0) U_1 \partial_\rho \eta_1 + M'(U_0) U_2 \partial_\rho \eta_0 + \frac{1}{2} M''(U_0) U_1^2 \partial_\rho \eta_0 \Big] \\ &\quad + \epsilon^2 \Big[M(U_0) \partial_\rho \eta_3 + M'(U_0) U_1 \partial_\rho \eta_2 + \Big(M'(U_0) U_2 + \frac{1}{2} M''(U_0) U_1^2 \Big) \partial_\rho \eta_1 \\ &\qquad + \Big(M'(U_0) U_3 + M''(U_0) U_1 U_2 + \frac{1}{6} M'''(U_0) U_1^3 \Big) \partial_\rho \eta_0 \Big] + O(\epsilon^3) \end{aligned} \tag{30}$$

which also justifies our expansion for $\mathbf{J}$.

3.3 Inner layer near the contact line

Moreover, concerning the inner layer about the contact line, let $\sigma(s,\tau)$ be the position of the free boundary in inner coordinates and consider coordinates centered about this free boundary, i.e. s and

$$z = \rho + \sigma(s,t). \tag{31}$$

The second inner expansions about the contact line may then be written as

$$\begin{aligned}\bar{U} &= 1 + \epsilon\bar{U}_1 + \epsilon^2\bar{U}_2..., \\ \bar{\eta} &= \bar{\eta}_0 + \epsilon\bar{\eta}_1 + \epsilon^2\bar{\eta}_2..., \\ \bar{\mathbf{J}} &= \epsilon^{-1}\bar{\mathbf{J}}_{-1} + \bar{\mathbf{J}}_0 + \epsilon\bar{\mathbf{J}}_1 + \epsilon^2\bar{\mathbf{J}}_2...\end{aligned}$$

and we postulate the boundary conditions

$$\bar{U}(0) = 1, \qquad \partial_z\bar{U}(0) = 0. \tag{32}$$

Note that since the position of the two inner layers as well depends on ϵ, the positions σ and R actually need to be expanded in terms of ϵ as well. But since we are only interested in the leading order behaviour of the interface we use σ and R and their leading order contributions interchangeably.
We now solve and match the outer and inner problems order by order.

3.4 Matching

3.4.1 Leading order

For the leading order outer problem we obtain

$$0 = \nabla\cdot\mathbf{j}_0, \qquad \mathbf{j}_0 = M(u_0)\nabla\mu_0, \qquad \mu_0 = F'(u_0), \tag{33}$$

and the corresponding boundary conditions are $\mathbf{m}\cdot\nabla u = 0$ and $\mathbf{m}\cdot\mathbf{j}_0 = 0$. Since we suppose that the "phase is outside the solid film, we conclude that

$$u_0 = -1, \qquad \mu_0 = 0. \tag{34}$$

The leading order inner expansion reads

$$\partial_\rho(M(U_0)\partial_\rho\eta_0) = 0, \tag{35a}$$

$$F'(U_0) - \partial_\rho\left(\gamma_0^2\partial_\rho U_0\right) = \eta_0. \tag{35b}$$

Integrating once in ρ, we obtain

$$M(U_0)\partial_\rho\eta_0 = a_1(s,\tau). \tag{36}$$

From the matching conditions we require

$$\lim_{\rho\to\infty} U_0(\rho) = -1, \tag{37}$$

which implies $a_1 \equiv 0$ and therefore also $\eta_0 = 0$. Moreover, from (27) we know that θ_0 is constant in ρ, which leads to

$$2(U_0^3 - U_0) - \gamma_0^2 \partial_{\rho\rho} U_0 = 0 \tag{38}$$

and, by applying the boundary condition $U_0(0) = 0$, consequently

$$U_0 = -\tanh\left(\frac{1}{\gamma_0}\rho\right). \tag{39}$$

Using $\eta_0 = 0$ we also conclude that

$$J_{n,-1} = 0. \tag{40}$$

Finally it is easily seen, that from the inner expansions about the contact line we get

$$\bar{U}_0 = 1, \qquad \bar{\eta}_0 = 0, \qquad \bar{J}_{n,-1} = 0. \tag{41}$$

$O(\epsilon)$ correction

The first two parts of the outer $O(\epsilon)$ correction problem for (18) are trivial, since $\mu_0 = 0$ and $M(u_0) = 0$ and consequently

$$\mathbf{j}_1 = 0. \tag{42}$$

The last equation becomes

$$\mu_1 = F''(u_0)u_1 = 4u_1, \tag{43}$$

which we need to match to η_1 in the following.
As $\eta_0 = 0$ we obtain for the first equation of the inner correction problem

$$\partial_\rho(M(U_0)\partial_\rho \eta_1) = 0, \tag{44}$$

such that $M(U_0)\partial_\rho \eta_1$ is constant in ρ. Comparison with (30) then reveals that (44) corresponds to the normal flux term $J_{n,0}$, which has to match with j_0 and consequently is zero. Thus η_1 does not depend on ρ.
Applying curvilinear coordinates the equation for η_1 reads

$$\begin{aligned}\eta_1 = F''(U_0)U_1 - \Big(&\mathbf{t}\partial_s\big(-\gamma_0\gamma_0'\mathbf{t}\partial_\rho U_0 + \gamma_0^2\mathbf{n}\partial_\rho U_0\big) + \mathbf{n}\partial_\rho\big(\gamma_0\gamma_0'\mathbf{n}\partial_s U_0 + \gamma_0^2\mathbf{t}\partial_s U_0\big)\\ &+ \mathbf{n}\partial_\rho\big(-(\gamma_1\gamma_0' + \gamma_0\gamma_1')\,\mathbf{t}\partial_\rho U_0 - \gamma_0\gamma_0'\mathbf{t}\partial_\rho U_1 + 2\gamma_0\gamma_1\mathbf{n}\partial_\rho U_0 + \gamma_0^2\mathbf{n}\partial_\rho U_1\big)\Big).\end{aligned} \tag{45}$$

Exploiting that $\gamma_0, \mathbf{n}$ and $\mathbf{t}$ do not depend on ρ, applying the two-dimensional Frenet-Serret formulae, i.e.

$$\partial_s \mathbf{t} = -\kappa\mathbf{n}, \qquad \partial_s \mathbf{n} = \kappa\mathbf{t},$$

and using the ρ-independence of θ_0 (see (27)) in order to calculate $\partial_s\gamma_0$, equation (45) becomes

$$\eta_1 = F''(U_0)U_1 - \kappa\big(\gamma_0'' + \gamma_0\big)\gamma_0\partial_\rho U_0 + \kappa\gamma_0'^2\partial_\rho U_0 + 2\kappa\gamma_0'^2\rho\partial_{\rho\rho}U_0 - \gamma_0^2\partial_{\rho\rho}U_1, \tag{46}$$

which reveals the ordinary differential equation

$$\gamma_0^2\partial_{\rho\rho}U_1 - 2(3U_0^2-1)U_1 = -\kappa c_1\gamma_0\partial_\rho U_0 + \kappa c_2\,\gamma_0\partial_\rho U_0 + 2\kappa c_2\,\gamma_0\rho\partial_{\rho\rho}U_0 - \eta_1, \quad (47)$$

where we substituted $c_1 := \gamma_0'' + \gamma_0$ and $c_2 := \frac{\gamma_0'^2}{\gamma_0}$. The general solution of (47) is given by

$$\begin{aligned} U_1 = {} & C_1\operatorname{sech}^2\left(\frac{\rho}{\gamma_0}\right) + C_2\operatorname{sech}^2\left(\frac{\rho}{\gamma_0}\right)\left(\frac{3\rho}{8\gamma_0} + \frac{1}{4}\sinh\left(\frac{2\rho}{\gamma_0}\right) + \frac{1}{32}\sinh\left(\frac{4\rho}{\gamma_0}\right)\right) \\ & + \frac{1}{8}(2c_1\kappa - \eta_1) + \frac{1}{48}(2c_1\kappa - 3\eta_1)\left(2\cosh\left(\frac{2\rho}{\gamma_2}\right) - 5\operatorname{sech}^2\left(\frac{\rho}{\gamma_0}\right)\right) \\ & - \frac{1}{2}c_2\kappa\left(\frac{\rho}{\gamma_0}\right)^2\operatorname{sech}^2\left(\frac{\rho}{\gamma_0}\right), \end{aligned} \quad (48)$$

and including the interface condition $U_1(0) = 0$ and boundedness as $\rho \to \infty$ to match with the outer solution, the two constants are given by

$$C_1 = -\frac{1}{16}(\eta_1 + 2c_1\kappa), \qquad C_2 = \frac{1}{3}(3\eta_1 - 2c_1\kappa). \quad (49)$$

Finally for the inner layer about the contact line we obtain $F''(\bar{U}_0) = 4$ and moreover $\partial_\rho\bar{U}_0 = 0$ leading to the ordinary differential equation

$$\eta_1 = 4\bar{U}_1 - \gamma_0^2\partial_{zz}\bar{U}_1, \quad (50)$$

with initial conditions

$$\bar{U}_1(0) = \bar{U}_1'(0) = 0. \quad (51)$$

The solution of (50) satisfying (51) is

$$\bar{U}_1 = \frac{\eta_1}{4}(1 - \cosh 2\bar{z}). \quad (52)$$

3.4.2 Exponential matching

We would now like to match the two interior layers. Since there are exponentially small and exponentially large terms in the expansions, which can not be matched by polynomial orders of ϵ we need to apply exponential matching as introduced by Lange [21].
As γ_0 is bounded everywhere, we denote $z = \rho/\gamma_0$ to simplify matters.
To match expansions about the interface and the contact point free boundary, we first note that as $\rho \to -\infty$

$$U_0 = 1 - 2e^{2z} + O(e^{4z}), \quad (53a)$$

$$U_1 = \frac{1}{24}(2c_1\kappa - 3\eta_1)e^{-2z} + \frac{1}{2}(c_1\kappa - \eta_1) \quad (53b)$$

$$+ \left[\left(\frac{7\eta_1}{4} - \frac{11c_1\kappa}{6}\right) + \left(\frac{3\eta_1}{2} - c_1\kappa\right)z - 2c_2\kappa z^2\right]e^{2z}. \quad (53c)$$

The inner expansion about the free boundary can be rewritten as

$$\bar{U} = 1 + \frac{\epsilon\eta_1}{4} - \frac{\epsilon\eta_1}{8}e^{2\bar{z}} - \frac{\epsilon\eta_1}{8}e^{-2\bar{z}} + O(\epsilon^2). \quad (54)$$

Consequently we find the matching condition

$$\frac{\eta_1}{4} = \frac{1}{2}(c_1\kappa - \eta_1) \quad \Rightarrow \quad \eta_1 = \frac{2}{3}c_1\kappa, \tag{55}$$

where $c_1 = \gamma_0'' + \gamma_0 > 0$.

$O(\epsilon^2)$ correction

Since $M'(u_0) = 0$ we obtain for the outer correction problem

$$\mathbf{n} \cdot \mathbf{j_2} = 0, \tag{56}$$

and again the first two parts of (18) are automatically satisfied. The last part requires

$$\mu_2 = \frac{1}{2}F'''(u_0)u_1^2 + F''(u_0)u_2, \tag{57}$$

where $F'''(u_0) = -12$ and $F''(u_0) = 4$.
Considering the inner correction problem and recalling that η_0, η_1 are independent of ρ we obtain for the first part of (18)

$$\partial_\rho(M(U_0)\partial_\rho\eta_2) = 0, \tag{58}$$

thus $M(U_0)\partial_\rho\eta_2$ is constant in ρ and since we can identify this expression via (30) as $J_{n,1}$ which has to match with $\mathbf{n} \cdot \mathbf{j}_1$ we find that

$$J_{n,1} = M(U_0)\partial_\rho\eta_2 = 0. \tag{59}$$

Therefore, η_2 is independent of ρ.

$O(\epsilon^3)$ correction

Consider the inner correction problem at this point. Since we have $M'(U_0) = M''(U_0) = 0$ we obtain from (30) that

$$J_{n,2} = M(U_0)\partial_\rho\eta_3. \tag{60}$$

For $\rho \to \infty$ the left hand side has to match with $\bar{J}_{n,2}$ and the right hand side with $\bar{\eta}_3$, but since the first case is zero and the second a constant we immediately obtain

$$\lim_{\rho\to-\infty} J_{n,2} = \lim_{\rho\to-\infty} M(U_0)\partial_\rho\eta_3 = 0 \tag{61}$$

Note that $J_{n,2}$ automatically matches with $\mathbf{n} \cdot \mathbf{j}_2|_{\chi_0}$ which is zero for $\rho \to \infty$, where χ_0 denotes the interface. Considering the last part of the correction problem for (18) and exploiting that η_0, η_1 and η_2 are independent of ρ we find

$$\begin{aligned} -v_n\partial_\rho U_0 &= \partial_\rho M(U_0)\partial_\rho + \partial_s M(U_0)\partial_s\eta_1 \\ &= \partial_\rho M(U_0)\partial_\rho + \frac{2}{3}M(U_0)\partial_{ss}(c_1\kappa). \end{aligned}$$

An integration over $(-\infty, \infty)$ then yields

$$v_n = \left(\frac{2}{3}\right)^2 \partial_{ss}(c_1\kappa). \tag{62}$$

Finally we obtain the sharp interface problem which correctly describes the anisotropic evolution due to surface diffusion

$$\begin{aligned} \mu_1 &= \frac{2}{3}c_1\kappa, \\ v_n &= \left(\frac{2}{3}\right)^2 \partial_{ss}((\gamma_0 + \gamma_0'')\kappa), \end{aligned} \tag{63}$$

on χ_0.

4 Sharp interface dynamics on solid boundaries

Now we would like to study the behavior of the anisotropic Cahn-Hilliard equation (18) in a local domain around the contact point x_0 with boundary condition (17b). Motivated by [27] we study the behaviour of u in a box around the contact point x_0. Introducing a boundary layer and an interior layer which imply corresponding matching conditions, we will show that the leading order system of (18) with boundary condition (17b) leads to a contact angle boundary condition, which is referred to Young-Herring condition in the literature [2, 23].

We first introduce the boundary layer near Γ_w

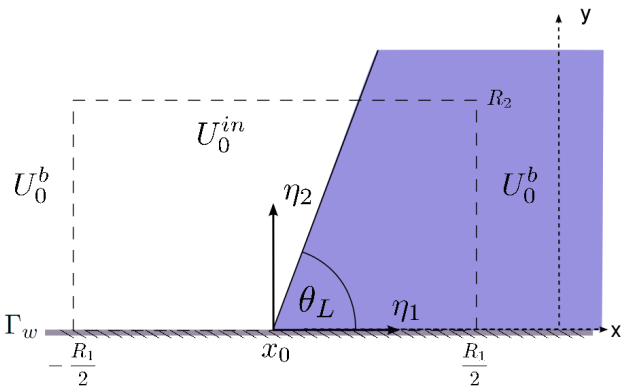

Figure 2: A sketch of the local domain.

$$z = \frac{y}{\epsilon}, \tag{64}$$

and expand $U^b(x, z)$ and μ_b into

$$\begin{aligned} U^b &= U_0^b + \epsilon U_1^b + \epsilon^2 U_2^b ..., \\ \mu^b &= \mu_0^b + \epsilon \mu_1^b + \epsilon^2 \mu_2^b .... \end{aligned} \tag{65}$$

Moreover we find for γ^b the expansion

$$\begin{aligned} \gamma^b &= \gamma(\theta_0^b) \quad + \epsilon\gamma'(\theta_0^b) + ... \\ &=: \quad \gamma_0^b \quad\quad + \epsilon\gamma_0^{b'} \quad + ... \end{aligned} \tag{66}$$

where

$$\theta_0^b = \lim_{\epsilon\to 0} \arctan 2\left(\partial_z U_0^b, \epsilon\partial_x U_0^b\right) = \begin{cases} +\frac{\pi}{2} & \text{, for } \partial_z U_0^b > 0 \\ -\frac{\pi}{2} & \text{, for } \partial_z U_0^b < 0 \\ 0 & \text{, for } \partial_z U_0^b = 0, \end{cases} \tag{67}$$

such that $\gamma_0 = \gamma(\theta_0)$ is piecewise constant and from Wulff's theorem (see Appendix D in [4]) we conclude that $\gamma(\frac{\pi}{2}) = -\gamma(-\frac{\pi}{2})$. The leading order problem of (18) then reads

$$0 = \partial_z\left(M(U_0^b)\partial_z\mu_0^b\right), \tag{68a}$$

$$\mu_0^b = F'(U_0^b) - \partial_z\left((\gamma_0^b)^2\partial_{zz}U_0^b\right), \tag{68b}$$

with boundary condition

$$(\gamma_0^b)^2\partial_z U_0^b = \frac{f_w'(U_0^b)}{\lambda} \qquad \text{, for } z = 0. \tag{68c}$$

Considering (68a) we first obtain that

$$a_1(\tau, x) = M(U_0^b)\partial_z\mu_b^0,$$

and conclude from the no-flux boundary condition at $z = 0$ that a_1 must be zero. This also implies $\mu_0^b = 0$ and consequently we obtain for (68b)

$$0 = F'(U_0^b) - \partial_z\left((\gamma_0^b)^2\partial_z U_0^b\right). \tag{69}$$

Multiplying by $\partial_z U_0^b$ and integrating over an arbitrary interval (z_1, z_2) we obtain

$$\int_{z_1}^{z_2} F'(U_0^b)\partial_z U_0^b\, dz = \int_{z_1}^{z_2} \partial_z\left((\gamma_0^b)^2\partial_z U_0^b\right)\partial_z U_0^b\, dz \tag{70}$$

which, since γ_0^b is piecewise constant and (z_1, z_2) is arbitrary, leads to

$$F(U_0^b) = \frac{1}{2}(\gamma_0^b)^2\left(\partial_z U_0^b\right)^2. \tag{71}$$

Next we introduce an interior layer centered at x_0. We choose inner coordinates which are stretched in both directions, i.e.

$$\eta_1 = \frac{x}{\epsilon}, \qquad \eta_2 = \frac{y}{\epsilon}, \tag{72}$$

and expand u and μ near $\eta = (\eta_1, \eta_2) = 0$ linearly as before

$$\begin{aligned} U^{in} &= U_0^{in} + \epsilon U_1^{in} + \epsilon^2 U_2^{in} ..., \\ \mu^{in} &= \mu_0^{in} + \epsilon\mu_1^{in} + \epsilon^2\mu_2^{in} .... \end{aligned} \tag{73}$$

Similar as before we have for γ^{in} the expansion

$$\begin{aligned} \gamma^{in} &= \gamma(\theta_0^{in}) \quad + \epsilon\gamma'(\theta_0^{in}) + ... \\ &=: \quad \gamma_0^{in} \quad + \epsilon\gamma_0^{in'} \quad + ... \end{aligned} \tag{74}$$

where now we have

$$\theta_0^{in} = \arctan 2 \left(\partial_{\eta_2} U_0^{in}, \partial_{\eta_1} U_0^{in}\right). \tag{75}$$

The leading order problem of (18) then reads

$$0 = \nabla \left(M(U_0^{in}) \nabla \mu_0^{in}\right), \tag{76a}$$

$$\mu_0^{in} = F'(U_0^{in}) - \nabla_\eta \left(\gamma_0^{in}\gamma_0^{in'} \begin{pmatrix} -\partial_{\eta_2} U_0^{in} \\ \partial_{\eta_1} U_0^{in} \end{pmatrix} + (\gamma_0^{in})^2 \nabla_\eta U_0^{in}\right), \tag{76b}$$

where similar as for (68a) we obtain that $\mu_0^{in} = 0$ and we have the leading order boundary condition

$$\gamma_0^{in}\gamma_0^{in'}\partial_{\eta_1} U_0^{in} + (\gamma_0^{in})^2 \partial_{\eta_2} U_0^{in} = \frac{f_w'(U_0^{in})}{\lambda} \qquad \text{, for } \eta_2 = 0. \tag{76c}$$

Consider now a box R of size R_1 in the η_1-direction and R_2 in the η_2 direction (see Fig. 2). Multiplying (76b) by $\partial_{\eta_1} U_0^{in}$ and integrating over R then leads to

$$\begin{aligned} \iint_R \partial_{\eta_1} U_0^{in} F'(U_0^{in}) = \iint_R \partial_{\eta_1} U_0^{in} \Big[&\partial_{\eta_1} \left(-\gamma_0^{in}\gamma_0^{in'}\partial_{\eta_2} U_0^{in} + (\gamma_0^{in})^2 \partial_{\eta_1} U_0^{in}\right) \\ &+ \partial_{\eta_2} \left(\gamma_0^{in}\gamma_0^{in'}\partial_{\eta_1} U_0^{in} + (\gamma_0^{in})^2 \partial_{\eta_2} U_0^{in}\right) \Big], \end{aligned} \tag{77}$$

which can be rewritten as

$$\begin{aligned} (\text{LHS}) &:= \iint_R \partial_{\eta_1} \left[F(U_0^{in}) + \frac{1}{2}(\gamma_0^{in})^2 \left(U_{0\eta_2}^{in}\right)^2 - \frac{1}{2}(\gamma_0^{in})^2 \left(U_{0\eta_1}^{in}\right)^2 + \gamma_0^{in}\gamma_0^{in'} U_{0\eta_1}^{in} U_{0\eta_2}^{in}\right] \\ &= \iint_R \partial_{\eta_2} \left[U_{0\eta_1}^{in} \left(\gamma_0^{in}\gamma_0^{in'} U_{0\eta_1}^{in} + (\gamma_0^{in})^2 U_{0\eta_2}^{in}\right)\right] =: (\text{RHS}) \end{aligned} \tag{78}$$

where we exploited that

$$\frac{1}{2}\partial_{\eta_1}(\gamma_0^{in})^2 = \gamma_0^{in}\gamma_0^{in'} \, \frac{U_{0\eta_2\eta_1}^{in} U_{0\eta_1}^{in} - U_{0\eta_1\eta_2}^{in} U_{0\eta_2}^{in}}{\left(U_{0\eta_1}^{in}\right)^2 + \left(U_{0\eta_2}^{in}\right)^2},$$

and used short forms, i.e. $U_{0\eta_1}^{in}$ for $\partial_{\eta_1} U_0^{in}$, to provide a better overview. We first consider the left-hand side (LHS) of (78), integrate in η_1 and apply $\lim_{|\eta_1|\to\infty} U_{0\eta_1}^{in} = 0$, which must be the case for finite energy solutions, which gives

$$\lim_{R_1,R_2\to\infty} (\text{LHS}) = \lim_{R_1\to\infty} \int_0^\infty \left[F(U_0^{in}) + \frac{1}{2}(\gamma_0^{in})^2 \left(U_{0\eta_2}^{in}\right)^2\right]_{-\frac{R_1}{2}}^{\frac{R_1}{2}} d\eta_2. \tag{79}$$

In order to match U_0^{in} with U_0^b for large η_1 we have the matching conditions

$$\begin{aligned} \lim_{\eta_1\to+\infty} U_0^{in} &= \lim_{x\to x_0^+} U_0^b(x,\eta_2) =: U_0^{b+}(x_0,\eta_2), \\ \lim_{\eta_1\to-\infty} U_0^{in} &= \lim_{x\to x_0^-} U_0^b(x,\eta_2) =: U_0^{b-}(x_0,\eta_2), \end{aligned} \tag{80}$$

where U_0^{b+} denotes the solution which is more on the side of the "+"phase and U_0^{b-} the solution which is more on the side of the "−"phase. Moreover, recalling (71) and (67) we obtain

$$U_{0\eta_2}^{b+} = \frac{1}{|\gamma_0^b|}\sqrt{2F(U_0^{b+})}, \qquad \text{and} \qquad U_{0\eta_2}^{b-} = -\frac{1}{|\gamma_0^b|}\sqrt{2F(U_0^{b-})}. \tag{81}$$

Without loss of generality we now assume that $U_{0\eta_2}^{b+/-} \neq 0$, for $\eta_2 \in [0,\infty)$, and find for (79)

$$\begin{aligned}\lim_{R_1,R_2\to\infty}(\text{LHS}) &= \int_0^\infty 2F(U_0^{b+}(x_0,\eta_2))\,d\eta_2 - \int_0^\infty 2F(U_0^{b-}(x_0,\eta_2))\,d\eta_2 \\ &= \sqrt{2}|\gamma_0^b|\left(\int_0^1 \sqrt{F(t)}\,dt + \int_0^{-1}\sqrt{F(t)}\,dt\right) \\ &= |\gamma_0^b|\left(\frac{2}{3}-\frac{2}{3}\right) \;=\; 0\end{aligned} \tag{82}$$

where we also applied the definition of $F(u) = \frac{1}{2}(1-u^2)^2$. Note that if $U_{0\eta_2}^{b+/-} = 0$ for some subset M_0 in $[0,\infty)$, the corresponding subinterval of (79) over M_0 would be zero anyway.

Considering the right hand side (RHS) of (78) we first obtain after integrating in η_2 and including the boundary condition (76c)

$$\begin{aligned}(\text{RHS}) &= \left[\int_{-R_1/2}^{R_1/2} U_{0\eta_1}^{in}\left(\gamma_0^{in}\gamma_0^{in\prime}U_{0\eta_1}^{in} + (\gamma_0^{in})^2 U_{0\eta_2}^{in}\right)\,d\eta_1\right]_0^{R_2} \\ &= \underbrace{\int_{-R_1/2}^{R_1/2} U_{0\eta_1}^{in}\left(\gamma_0^{in}\gamma_0^{in\prime}U_{0\eta_1}^{in} + (\gamma_0^{in})^2 U_{0\eta_2}^{in}\right)\,d\eta_1\Big|_{R_2}}_{\text{I}} - \underbrace{\int_{-R_1/2}^{R_1/2} U_{0\eta_1}^{in}\frac{f_w'(U_0^{in})}{\lambda}\,d\eta_1}_{\text{II}}\end{aligned}$$

where (II) in the limit $R_1, R_2 \to \infty$ is

$$\lim_{R_1,R_2\to\infty}(\text{II}) = \frac{1}{\lambda}\int_{-1}^{1} f_w'(t)\,dt = \frac{1}{\lambda}(\gamma_{FS}-\gamma_{VS}). \tag{83}$$

Analysing (I) we continue by transforming into curvilinear coordinates (see Fig. 3) for which we have the relation

$$\begin{aligned}\xi &= -\eta_1\sin\theta_L \;+\; \eta_2\cos\theta_L \\ \chi &= \;\;\eta_1\cos\theta_L \;+\; \eta_2\sin\theta_L\end{aligned} \tag{84}$$

and consequently

$$\begin{aligned}\partial_{\eta_1} &= -\sin\theta_L\partial_\xi \;+\; \cos\theta_L\partial_\chi \\ \partial_{\eta_2} &= \;\;\cos\theta_L\partial_\xi \;+\; \sin\theta_L\partial_\chi.\end{aligned} \tag{85}$$

Here $\theta_L \in (0,\pi)$ denotes the contact angle on the right hand side of the thin solid film which has negative sign due to the geometric orientation (see Fig. 3). The transformed integral then reads

$$(\text{I}) = \int_{\frac{R_1}{2}\sin\theta_L + R_2\cos\theta_L}^{-\frac{R_1}{2}\sin\theta_L + R_2\cos\theta_L} S\,d\xi \tag{86}$$

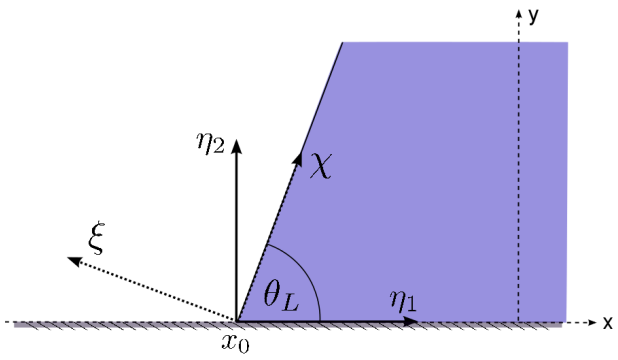

Figure 3: A sketch of the coordinate transformation.

where

$$\begin{aligned} S =& \gamma_0^{in}\gamma_0^{in\prime}\left(-\sin\theta_L\left(U_{0\xi}^{in}\right)^2 + 2\cos\theta_L U_{0\xi}^{in}U_{0\chi}^{in} - \frac{\cos^2\theta_L}{\sin\theta_L}\left(U_{0\chi}^{in}\right)^2\right) \\ &+ (\gamma_0^{in})^2\left(\cos\theta_L\left(U_{0\xi}^{in}\right)^2 + \left(\sin\theta_L - \frac{\cos^2\theta_L}{\sin\theta_L}\right)U_{0\xi}^{in}U_{0\chi}^{in} - \cos\theta_L\left(U_{0\chi}^{in}\right)^2\right) \end{aligned} \tag{87}$$

Now, $R_1 \gg 1$ and $R_2 \gg 1$ implies $\chi \gg 1$ and therefore $\lim_{\chi\to\infty}\partial_\chi U_0^{in} = 0$. Taking the limit $R_1 \to \infty, R_2 \to \infty$ in the following way:

$$\lim_{R_1,R_2\to\infty}(\mathrm{I}) = \lim_{\substack{\alpha\to\infty \\ |R_1\sin\theta_L + R_2\cos\theta_L| < \alpha}} \lim_{\substack{R_1\to\infty \\ R_2\to\infty}} \int_{\frac{R_1}{2}\sin\theta_L + R_2\cos\theta_L}^{-\frac{R_1}{2}\sin\theta_L + R_2\cos\theta_L} S\, d\xi \tag{88}$$

leads to

$$\lim_{R_1,R_2\to\infty}(\mathrm{I}) = -\left(-\gamma_0^{in}\gamma_0^{in\prime}\sin\theta_L + \left(\gamma_0^{in}\right)^2\cos\theta_L\right)\int_{-\infty}^{\infty}\left(U_{0\xi}^{in}\right)^2\, d\xi \tag{89}$$

where we applied that

$$\lim_{\chi\to\infty}\gamma_0^{in} = \gamma_0^{in}(\arctan 2\left(\cos\theta_L, -\sin\theta_L\right)) = \gamma_0 \tag{90}$$

and consequently γ_0^{in} is constant in χ and ξ. Moreover note that (90) reveals, that γ_0^{in} is equivalent to γ_0 from Section 3.2. Finally we obtain by once more using (71) and

$$U_{0\xi}^{in} = -\frac{1}{\gamma_0}\sqrt{2F(U_0^{in})}, \tag{91}$$

that

$$\begin{aligned} \int_{-\infty}^{\infty}\left(U_{0\xi}^{in}\right)^2\, d\xi &= \frac{2}{\gamma_0^2}\int_{-\infty}^{\infty}F(U_0^{in})\, d\xi \\ &= -\frac{\sqrt{2}}{\gamma_0}\int_1^{-1}\sqrt{F(t)}\, dt \quad = \quad \frac{1}{\gamma_0}\frac{4}{3}. \end{aligned} \tag{92}$$

All together we obtain by merging the results for (LHS) and (RHS) in (78)

$$0 = \frac{4}{3}\left(-\gamma_0{}'\sin\theta_L + \gamma_0\cos\theta_L\right) - \frac{1}{\lambda}(\gamma_{VS} - \gamma_{FS}) \tag{93}$$

which is, up to scalars, the correct surface- energy minimizing equilibrium contact angle boundary condition, referred to as Young-Herring condition [23]. Note that if we consider the contact angle on the right hand side θ_R, where $\sin\theta_R < 0$ due to the geometric orientation, we obtain in an analogous way the same equation which suggests to rewrite (93) in general form

$$0 = \frac{4}{3}\left(-{\gamma_0}'\sin\theta_C + \gamma_0\cos\theta_C\right) - \frac{1}{\lambda}(\gamma_{VS} - \gamma_{FS}), \tag{94}$$

for $\theta_C \in (0,\pi)$. If the surface energy is isotropic, i.e. $\gamma \equiv$ const. equation (94) reduces to the well- known Young's equation. Moreover we would like to remark, that in the case of weak anisotropy, i.e. $\gamma + \gamma'' > 0$, which is provided by this paper, equation (94) has a unique solution θ_C. In order to observe the number of possible choices for θ_C it is convenient to consider (94) as a function of θ, i.e.

$$h(\theta) := \frac{4}{3}\left(-{\gamma_0}'\sin\theta + \gamma_0\cos\theta\right) - \frac{1}{\lambda}(\gamma_{VS} - \gamma_{FS}) \tag{95}$$

and determine the number of zeros. Differentiating with respect to θ reveals

$$h'(\theta) := -\frac{4}{3}\left({\gamma_0}'' + \gamma_0\right)\sin\theta \tag{96}$$

which is always negative for weak anisotropy and $\theta \in (0,\pi)$ such that $h(\theta)$ is strictly monotonically decreasing and can only have one zero in this interval.

5 Conclusion

In the present work we investigated a phase-field model describing the dewetting from a solid substrate. The main goal was to establish the connection to a corresponding sharp-interface model that accounts for surface diffusion as the dominant mechanism that drives the dynamics. The focus of this study was the systematic and careful asymptotic analysis to treat the multiple boundary and interfacial layers that occur as the sharp-interface limit is approached, both for the isotropic as well as for the anisotropic case.

We established that by using exponential asymptotic matching the bi-quatratic mobility yields the correct limiting model, in contrast to for example other choices such as $M(u) = 1 - u^2$, which have been used before in the literature, see for example Jiang et al. [16] in this context of application. Such mobilities lead to sharp-interface models that contain bulk diffusion as an additional driving force to the same order of magnitude, as previously shown by Lee et al. [22].

A further problem concerned the asymptotics of the contact-line motion as the solid substrate is approached. For this the outer problem has to be matched to the boundary layer near the solid substrate and moreover it had to match the interior interfacial layer. As a result the Young-Herring condition is obtained.

For comparison to realistic scenarios and experimental results of dewetting solid films, such as dewetting crystalline Si films, used for nanopatterning of surfaces, our phase-field model will be extended to a higher dimension and and investigated numerically in

an upcoming separate article. Of interest is here the study of the solid-solid contact-line instability, which, according to experimental results by [11], seems to be a function of the crystalline orientation.

References

[1] Oliver Bäumchen, Ludovic Marquant, Ralf Blossey, Andreas Münch, Barbara Wagner, and Karin Jacobs. Influence of slip on the Rayleigh-Plateau rim instability in dewetting viscous films. *Physical Review Letters*, 113:014501, 2014.

[2] S. Bottin-Rousseau, M. Serefoglu, S. Akamatsu, and G. Faivre. The surface tension force of anisotropic interphase boundaries is perpendicular to the solidification front during eutectic growth. *IOP Conf. Series: Materials Science and Engineering*, 27:012088, 2011.

[3] L. Bronsard and F. Reitich. On three-phase boundary motion and the singular limit of a vector-valued ginzburg-landau equation. *Arch. Rat. Mech. Anal.*, 124:355–379, 1993.

[4] W.K. Burton, N. Cabrera, and F.C. Frank. The growth of crystals and the equilibrium structure of their surfaces. *Phil. Trans. Roy. Soc. Lond.*, 243:299–358, 1951.

[5] J. W. Cahn and J. E. Taylor. Surface motion by surface diffusion. *Acta Metall. Mater.*, 42(4):1045–1063, April 1994.

[6] J.W. Cahn, C.M. Elliott, and A. Novick-Cohen. The cahn-hilliard equation with a concentration dependent mobility: motion by minus the laplacian of the mean curvature. *Europ. Jour. Appl. Math.*, 7:287–302, 1996.

[7] R. V. Craster and O. K. Matar. Dynamics and stability of thin liquid films. *Rev. Mod. Phys.*, 81:1131–1198, Aug 2009.

[8] David T. Danielson, Daniel K. Sparacin, Jürgen Michel, and Lionel C. Kimerling. Surface-energy-driven dewetting theory of silicon-on-insulator agglomeration. *Journal of applied physics*, 100:083507, 2006.

[9] P. G. de Gennes. Wetting: statics and dynamics. *Rev. Mod. Phys.*, 57:827–863, 1985.

[10] E. Dornel, J-C. Bare, F. de Crecy, and G. Lacolle. Surface diffusion dewetting of thin solid films: Numerical method and application to si/ sio2. *Phys. Rev. B*, 73:115427, 2006.

[11] M. Dufay and O. Pierre-Louis. Anisotropy and coarsening in the instability of solid dewetting fronts. *Phys. Rev. Lett.*, 106(10):105506, 2011.

[12] J.J. Eggleston, G.B. McFadden, and P. W. Voorhees. A phase-field model for highly anisotropic interfacial energy. *Phys. D*, 150:91–103, 2001.

[13] C. Guggenberger, Robert Spatschek, and Klaus Kassner. Comparison of phase-field models for surface diffusion. *Phys. Rev. E*, 78:016703, 2008.

[14] Mathew G. Hennessy, Victor M. Burlakov, Andreas Münch, Alain Goriely, and Barbara Wagner. Controlled topological transitions in thin film phase separation. *WIAS preprint 1885*, 2013.

[15] D. Jacqmin. Contact-line dynamics of a diffuse fluid interface. *J. Fluid Mech.*, 402:57–88, 2000.

[16] Wei Jiang, Weizhu Bao, Carl V. Thompson, and David J. Srolovitz. Phase field approach for simulating solid-state dewetting problems. *Acta Mater.*, 60:5578–5592, 2012.

[17] E. Jiran and C. V. Thompson. Capillary instabilities in thin films. *Journal of Electronic Materials*, 19(11):1153–1160, November 1990.

[18] J. R. King, A. Münch, and B. Wagner. Linear stability analysis of a sharp-interface model for dewetting thin films. *J. Engrg. Math.*, 63:177–195, 2009.

[19] Ryo Kobayashi. Modeling and numerical simulations of dendritic crystal growth. *Physica D*, 63:410–423, 1993.

[20] M. D. Korzec, M Roczen, M. Schade, B. Wagner, and B. Rech. Equilibrium shapes of polycrystalline silicon nanodots. *J. Appl. Phys.*, 115:(074304) 1–13, 2014.

[21] C. G. Lange. On spurious solutions of singular perturbation problems. *Studies Appl. Math.*, 68:227–257, 1983.

[22] Alpha Albert Lee, Andreas Münch, and Endre Süli. Sharp interface limits of the cahn-hilliard equation with degenerate mobility. *unknown*, unknown:unknown, unknown.

[23] D. Min and H. Wong. The effect of strong surface energy anisotropy on migrating grain-boundary grooves. *Jour. Appl. Phys.*, 100:053523, 2006.

[24] W. W. Mullins and R. F. Sekerka. Morphological stability of a particle growing by diffusion or heat flow. *Jour. Appl. Phys.*, 34:323–329, 1963.

[25] A. Novick-Cohen. Triple-junction motion for an allenâĂŞcahn/cahnâĂŞhilliard system. *Physica D*, 137:1–24, 2000.

[26] A. Novick-Cohen. The cahn-hilliard equation. *Handbook of differential equations: evolutionary equations*, 4:931, 2008.

[27] N.C. Owen, J. Rubinstein, and P. Sternberg. Minimizers and gradient flows for singularly perturbed bi-stable potentials with a dirichlet dondition. *Proc. R. Soc. Lond. A*, 429:505–532, 1990.

[28] Robert L. Pego. Front migration in the nonlinear cahn-hilliard equation. *Proc. Roy. Soc. Lond.*, 422:261– 278, 1989.

[29] Sanjay Puri and Kurt Binder. Surface effects on spinodal decomposition in binary mixtures and the interplay with wetting phenomena. *Physical Review E*, 49:5359, 1994.

[30] Francesco Ruffino and M. G. Grimaldi. Self-organized patterned arrays of au and ag nanoparticles by thickness-dependent dewetting of template-confined films. *Journal of Materials Science*, 49:5714–5729, 2014.

[31] D. N. Sibley, A. Nold, and S. Kalliadasis. Unifying binary fluid diffuse-interface motion laws in the sharp-interface limit. *Jour. Fluid Mech.*, 736:5–43, 2013.

[32] J.E. Taylor and J.W. Cahn. Linking anisotropic sharp and diffuse surface motion laws via gradient flows. *Jour. Stat. Phys.*, 77:183–197, 1994.

[33] J.E. Taylor and J.W. Cahn. Diffuse interfaces with sharp corners and facets: Phase field models with strongly anisotropic surfaces. *Physica D*, 112:381–411, 1998.

[34] C. V. Thompson. Solid-state dewetting of thin films. *Annu. Rev. Mater. Res.*, 42:399–434, 2012.

[35] C. V. Thompson and J. Ye. Mechanisms of complex morphological evolution during solid-state dewetting of single-crystal nickel thin films. *Appl. Phys. Let*, 97:071904, 2010.

[36] C. V. Thompson and J. Ye. Anisotropic edge retraction and hole growth during solid-state dewetting of single crystal nickel thin films. *Acta Mat.*, 59:582–589, 2011.

[37] W. L. Winterbottom. Equilibrium shape of a small particle in contact with a foreign substrate. *Acta Metall.*, 15:303–310, 1967.

[38] S. Wise, J. Kim, and J. Lowengrub. Solving the regularized, strongly anisotropic cahn-hilliard equation by an adaptive nonlinear multigrid method. *Jour. Comp. Phys.*, 226:414–446, 2007.

[39] H. Wong, P. W. Vorhees, M. J. Miksis, and S. H. Davis. Periodic mass shedding of a retracting solid film step. *Acta Mater.*, 48:1719–1728, 2000.

[40] T. Young. An essay on the cohesion of fluids. *Philos. Trans. Roy. Soc. London*, 95:65–87, 1805.

[41] Pengtao Yue, Chunfeng Zhou, and J.J. Feng. Sharp-interface limit of the cahn-hilliard model for moving contact-lines. *J. Fluid Mech.*, 645:279–294, 2010.

[42] R.V. Zucker, G. H. Kim, W. C. Carter, and C. V. Thompson. A model for solid-state dewetting of a fully-faceted thin film. *C. R. Phys.*, 14:564–577, 2013.